Quasi-static electromagnetic fields created by an electric dipole in the vicinity of a dielectric sphere: method of images

Jorge R. Zurita-Sánchez
Instituto Nacional de Astrofísica, Óptica y Electrónica,
Apartado Postal 51, Puebla, Pue. 72000, México.

Recibido el 1 de junio de 2009; aceptado el 15 de octubre de 2009

We present a quasi-static description of the electromagnetic fields created by an oscillating electric dipole in the vicinity of a dielectric sphere. In this description: the fields are generated by image sources, a simple physical picture of the electromagnetic response of the dipole nearby a dielectric sphere is obtained, and the nearfields are calculated from the Green tensor of a bulk medium. This quasi-static description can be applied to study radiative properties of emitters (molecules, atoms, etc.) placed in the vicinity of a dielectric spherical nanoparticle.

Keywords: Electric dipole radiation; dielectric sphere.

Se presenta una descripción cuasi-estática de los campos electromagnéticos creados por un dipolo eléctrico que oscila en la cercanía de una esfera dieléctrica. En esta descripción, los campos son generados por fuentes imagen, se obtiene una representación física simple de la respuesta electromagnética del dipolo cercano a la esfera dieléctrica y los campos cercanos se obtienen a partir del tensor de Green para un medio ilimitado. Esta descripción cuasi-estática puede ser aplicada en el estudio de las propiedades radiativas de emisores (moléculas, átomos, etc.) localizados en la cercanía de una nanopartícula esférica.

Descriptores: Radiación de un dipolo eléctrico; esfera dieléctrica.

PACS: 03.50.De; 41.20.-q

1. Introduction

We focus on the electromagnetic fields created by an oscillating electric dipole in the vicinity of a dielectric sphere. Although an exact treatment for the fields created by an electric dipole placed near a sphere already exists [1], our quasi-static description will ease the analytical description and provide a simple physical picture. As might be expected this description approximates well the fields inside the volume λ^3 [λ being the wavelength of the radiation] that encloses the dipole and the sphere. In our quasi-static description, the electromagnetic fields are generated by image sources. Therefore, the finding of these sources is our central objective. A static image description for a single charge in presence of a dielectric sphere has been obtained by Lindell [2]. Based on his methodology, we derive the image sources for the case of an electric dipole.

The radiative properties of a emitter (molecule, atom, quantum dot, nano-antenna, etc.) depend on the environment in which it is embedded. The study of the influence of nearby nano-objects on these radiative properties is important. For example, near-field techniques rely precisely on the optical response of a sample placed in the vicinity of subwavelength apertures and sharp tips [3, 4], the modification of the lifetime and the fluorescence rate of a molecule in presence of a nano-particle [1, 5–9]. Our approach can be applied to the study of certain radiative properties of emitters placed in the vicinity of nanoscale spheres. The reason is that most of such emitters have a characteristic wavelength lying in the visible spectrum which is larger than the length of a nanostructure.

The paper is organized as follows. In Sec. 2, we derive the image charge and current densities arising from the electric dipole oriented in the radial and tangential directions. Sec. 3 establishes the expressions to obtain the electric field created by the image distributions that are found in previous section. Next, Sec. 4 is devoted to the discussion of the quasi-static picture. Also, this section shows plots of the electric field generated by a dipole for particular cases. Finally, the conclusions are presented in Sec. 5.

2. Image sources

We consider a sphere with radius a and dielectric constant ϵ_a that is centered at the origin. Outside the sphere, the medium has a dielectric constant ϵ_b and an electric dipole with moment p is located at $\mathbf{r}_d = z_o\mathbf{n}_z$ [$\mathbf{n}_z$ is the unit vector in the z-direction]. Due to the geometry, the electromagnetic response of an arbitrarily oriented dipole can be reduced as the superposition of the responses of the dipole for the tangential ($\mathbf{n}_x$) and radial ($\mathbf{n}_z$) directions [$\mathbf{n}_x$ is the unit vector in the x-direction].

2.1. Tangential orientation

2.1.1. Outside the sphere

The electrostatic potential *outside* the sphere created by the dipole is

$$\Phi_{\text{out}\|}(r,\theta,\phi) = \Phi_{\text{f}}(\mathbf{r}) + \Phi_{\|1}(r,\theta,\phi). \tag{1}$$

Here, Φ_{f} is the potential created by the dipole in the absence of sphere,

$$\Phi_{\text{f}}(\mathbf{r}) = \frac{1}{4\pi\varepsilon_o\epsilon_b}\frac{\mathbf{p}\cdot\mathbf{R}}{|\mathbf{R}|^3}, \tag{2}$$

and $\Phi_{\|1}$ is the potential arising from the induced charge distribution in the sphere which is explicitly expressed as [10]

$$\Phi_{\|1}(r,\theta,\phi) = -p\frac{\cos\phi}{4\pi\varepsilon_o\epsilon_b} \times \sum_{n=1}^{\infty} \frac{(\epsilon_a-\epsilon_b)n}{(\epsilon_a+\epsilon_b)n+\epsilon_b} b^n \frac{a}{z_o^2}\frac{P_n^1(\cos\theta)}{r^{n+1}}. \quad (3)$$

Here, ε_o is the vacuum permittivity, $\mathbf{R} = \mathbf{r} - \mathbf{r}_\mathrm{d}$, (r,θ,ϕ) are the spherical coordinates,

$$b \equiv a^2/z_o,$$

and P_n^1 is the associated Legendre polynomial of order n [see Eq. (A.5)]. Our aim is to find an image charge distribution embedded in medium ϵ_b that generates the same potential as in Eq. (3). We assume that the image charge density has the form

$$\rho_{\|1}(x,y,z) = \left[\frac{d}{dx}\delta(x)\right]\delta(y)g_{\|1}(z), \quad (4)$$

where $\delta(\ldots)$ is the Dirac-δ function, and $g_{\|1}(z)$ is the function to be determined. Since the charge density of a point dipole is proportional to the spatial derivative of a Dirac-δ function, the charge density $\rho_{\|1}(x,y,z)$ [Eq. (4)] can be seen as a line of dipoles along the z-axis that are oriented in the x-direction. Moreover, the charged line extends from the center of the sphere to $z = a$. From these assumptions, the potential created by $\rho_{\|1}$ is

$$\Phi_{\|1}(r,\theta,\phi) = \int_{V'} \frac{\rho(x',y',z')}{4\pi\varepsilon_o\epsilon_b|\mathbf{r}-\mathbf{r}'|}dV'$$

$$= -\frac{r\sin\theta\cos\phi}{4\pi\varepsilon_o\epsilon_b}\int_0^a \frac{g_{\|1}(z')}{(r^2-2rz'\cos\theta+z'^2)^{3/2}}dz'. \quad (5)$$

By using the fact that [11]

$$\frac{1}{(1-2uv+v^2)^{3/2}} = \sum_{n=1}^{\infty}\frac{v^{n-1}}{\sqrt{1-u^2}}P_n^1(u), \qquad |v|<1, \quad (6)$$

and setting $u = \cos\theta$ and $v = z'/r$, Eq. (5) becomes

$$\Phi_{\|1}(r,\theta,\phi) = -\frac{\cos\phi}{4\pi\varepsilon_o\epsilon_b}\sum_{n=1}^{\infty} b^{n-1}\frac{P_n^1(\cos\theta)}{r^{n+1}} \times \int_0^a g_{\|1}(z')\left[\frac{z'}{b}\right]^{n-1}dz'. \quad (7)$$

By comparing Eqs. (3) and (7), we obtain that $g_{\|1}(z)$ must fulfill

$$\int_0^a g_{\|1}(z')\left[\frac{z'}{b}\right]^{n-1}dz' = p\frac{a^3}{z_o^3}\frac{\epsilon_a-\epsilon_b}{\epsilon_a+\epsilon_b}\frac{n}{n+\alpha}, \qquad n = 1,2,\ldots, \quad (8)$$

where α is

$$\alpha \equiv \epsilon_b/(\epsilon_a+\epsilon_b). \quad (9)$$

It turns out that

$$g_{\|1}(z) = p\frac{a^3}{z_o^3}\frac{\epsilon_a-\epsilon_b}{\epsilon_a+\epsilon_b}\delta(z-b) - p\frac{a}{z_o^2}\frac{\epsilon_b(\epsilon_a-\epsilon_b)}{(\epsilon_a+\epsilon_b)^2}\left(\frac{z}{b}\right)^{\alpha}\Theta(b-z) \quad (10)$$

satisfies Eq. (8), where $\Theta(\ldots)$ is the step function. $g_{\|1}(z)$ given by Eq. (10) is valid for $1+\alpha > 0$.

If the electric dipole oscillates with angular frequency ω as $\mathbf{p} = p\mathbf{n}_x\exp(-\mathrm{i}\omega t)$, then it induces a density current in the x-direction, that is, $\mathbf{j}_{\|1}(\mathbf{r},\omega) = j_{\|1}(\mathbf{r},\omega)\mathbf{n}_x$. By using the continuity equation $[\partial j_{\|1}(\mathbf{r},\omega)/\partial x = \mathrm{i}\omega\rho_{\|1}(\mathbf{r},\omega)]$ and Eq. (4), the density current in the quasi-static approximation becomes

$$j_{\|1}(\mathbf{r},\omega) \quad = \quad \mathrm{i}\omega\delta(x)\delta(y)g_{\|1}(z). \quad (11)$$

We notice that the current density [Eq. (11)] is constituted by: (1) a single dipole that is located at $b\mathbf{n}_z$ and is oriented in the x-direction, and (2) a set of dipoles that are placed in the line from $z = 0$ to $z = b$ and oriented in the x-direction [see Fig. 1].

2.1.2. *Inside the sphere*

Now, we turn to the case for the potential inside the sphere that originated from the presence of the dipole. This potential is (see Appendix A)

$$\Phi_{\|2}(r,\theta,\phi) = p\frac{\cos\phi}{4\pi\varepsilon_o\epsilon_a} \times \sum_{n=1}^{\infty}\frac{\epsilon_a(2n+1)}{(\epsilon_a+\epsilon_b)n+\epsilon_b}\frac{r^n}{z_o^{n+2}}P_n^1(\cos\theta). \quad (12)$$

Similarly to the previous case, we look for a charge distribution $\rho_{\|2}$ now embedded in medium ϵ_a which creates the same potential as Eq. (12). Also, we consider that the image charge distribution $\rho_{\|2}$ is a line of dipoles which are oriented in the x-direction, but the charged line extends from $z = a$ to $z \to \infty$. Thus, $\rho_{\|2}$ takes the same form as in Eq. (4), but $g_{\|2}(z)$ replaces $g_{\|1}(z)$ and the integral runs along the aforementioned line. It follows that the potential created by $\rho_{\|2}$ is

$$\Phi_{\|2}(r,\theta,\phi) = -\frac{r\sin\theta\cos\phi}{4\pi\varepsilon_o\epsilon_a} \times \int_a^{\infty}\frac{g_{\|2}(z')}{(r^2-2rz'\cos\theta+z'^2)^{3/2}}dz'. \quad (13)$$

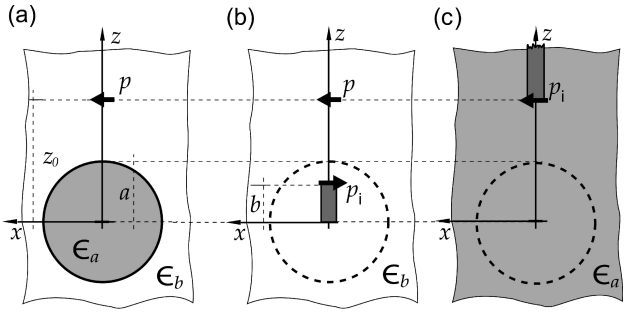

FIGURE 1. (a) An electric dipole p is oriented along the x-axis and located a distance z_o from the center of the sphere with radius a and dielectric constant ϵ_a. (b) The image distribution (embedded in medium ϵ_b) for the field outside the sphere is composed of a dipole and a line of dipoles. (c) The image distribution (embedded in medium ϵ_a) for the field inside the sphere is composed of a dipole and a line of dipoles.

By using Eq. (6) with $u = \cos\theta$ and $v = r/z'$, Eq. (13) becomes

$$\Phi_{\|2}(r,\theta,\phi) = -\frac{\cos\phi}{4\pi\varepsilon_o\epsilon_a}\sum_{n=1}^{\infty} P_n^1(\cos\theta)\frac{r^n}{z_o^{n+2}} \times \int_a^{\infty} g_{\|2}(z')\left[\frac{z_o}{z'}\right]^{n+2} dz'. \quad (14)$$

A comparison of Eqs. (12) and (14) shows that $g_{\|2}(z)$ must fullfill

$$\int_a^{\infty} g_{\|2}(z')\left[\frac{z_o}{z'}\right]^{n+2} dz' = -p\frac{2\epsilon_a}{\epsilon_a+\epsilon_b}\frac{n+1/2}{n+\alpha}, \quad n=1,2,\ldots \quad (15)$$

Then, it is found that the solution of Eq. (15) is

$$g_{\|2}(z) = -p\,\frac{2\epsilon_a}{\epsilon_a+\epsilon_b}\delta(z-z_o) - p\frac{\epsilon_a(\epsilon_a-\epsilon_b)}{(\epsilon_a+\epsilon_b)^2}\Theta(z-z_o)\frac{z}{z_o^2}\left(\frac{z_o}{z}\right)^{\alpha}. \quad (16)$$

Also, $g_{\|2}(z)$ given in Eq. (16) is valid for $1+\alpha > 0$.

As the dipole oscillates with angular frequency ω, the induced current density that is oriented in the x-direction becomes

$$j_{\|2}(\mathbf{r},\omega) = \mathrm{i}\omega\delta(x)\delta(y)g_{\|2}(z). \quad (17)$$

As can be seen, the current density [Eq. (17)] arises from: (1) a single dipole that is located at $z_o\mathbf{n}_z$, and (2) a set of dipoles that are placed at the line from $z = z_o$ to $z \to \infty$. All of them are oriented in the x-direction [see Fig. 1c].

2.2. Radial orientation

2.2.1. *Outside the sphere*

Similarly to Eq. (1), the potential outside the sphere for the radial orientation is

$$\Phi_{\text{out}\perp}(r,\theta,\phi) = \Phi_{\text{f}}(\mathbf{r}) + \Phi_{\perp 1}(r,\theta), \quad (18)$$

namely, the addition of the potential in absence of the sphere and the potential created by the induced charge distribution in the sphere. The latter is [10]

$$\Phi_{\perp 1}(r,\theta) = \frac{p}{4\pi\varepsilon_o\epsilon_b} \times \sum_{n=0}^{\infty}\frac{(\epsilon_a-\epsilon_b)n(n+1)}{(\epsilon_a+\epsilon_b)n+\epsilon_b} b^n\frac{a}{z_o^2}\frac{P_n(\cos\theta)}{r^{n+1}}, \quad (19)$$

where $P_n(\ldots)$ is the Legendre polynomial of order n. Now, we assume that the image charge density has the form

$$\rho_{\perp 1}(x,y,z) = \delta(x)\delta(y)h_{\perp 1}(z). \quad (20)$$

Also, we consider that the charge extends from $z = 0$ to $z = a$. Thus, the potential created by $\rho_{\perp 1}$ is

$$\Phi_{\perp 1}(r,\theta) = \frac{1}{4\pi\varepsilon_o\epsilon_b} \times \int_0^a \frac{h_{\perp 1}(z')}{(r^2-2rz'\cos\theta+z'^2)^{1/2}}dz'. \quad (21)$$

By the fact that

$$\frac{1}{(1-2uv+v^2)^{1/2}} = \sum_{n=0}^{\infty} v^n P_n(u), \qquad |v|<1, \quad (22)$$

with $u = \cos\theta$ and $v = z'/r$, Eq. (21) can be expressed as

$$\Phi_{\perp 1}(r,\theta) = \frac{1}{4\pi\varepsilon_o\epsilon_b} \times \sum_{n=0}^{\infty} b^n\frac{P_n(\cos\theta)}{r^{n+1}}\int_0^a h_{\perp 1}(z')\left[\frac{z'}{b}\right]^n dz'. \quad (23)$$

By comparing Eqs. (19) and (23), $h_{\perp 1}(z)$ must fulfill

$$\int_0^a h_{\perp 1}(z')\left[\frac{z'}{b}\right]^n dz' = p\frac{a}{z_o^2}\frac{\epsilon_a-\epsilon_b}{\epsilon_a+\epsilon_b}\frac{n(n+1)}{n+\alpha}, \qquad n=0,1,2,\ldots \quad (24)$$

It follows that Eq. (24) is satisfied if

$$h_{\perp 1}(z) = \frac{d}{dz}g_{\perp 1}(z), \quad (25)$$

$$g_{\perp 1}(z) \equiv -p\frac{a^3}{z_o^3}\frac{\epsilon_a-\epsilon_b}{\epsilon_a+\epsilon_b}r_1(z)\delta(z-b) - p\frac{a}{z_o^2}\frac{\epsilon_a(\epsilon_a-\epsilon_b)}{(\epsilon_a+\epsilon_b)^2}\left(\frac{z}{b}\right)^{\alpha}\Theta(b-z), \quad (26)$$

$$r_1(z) = (z/b)^{\alpha+1}. \quad (27)$$

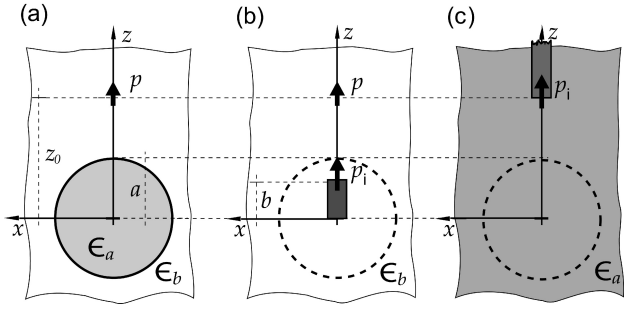

FIGURE 2. (a) An electric dipole p is oriented along the z-axis and located at a distance z_o from the center of the sphere having radius a and dielectric constant ϵ_a. (b) The image distribution (embedded in medium ϵ_b) for the field outside the sphere is composed of a dipole and a charged line. (c) The image distribution (embedded in medium ϵ_a) for the field inside the sphere is composed of a dipole and a charged line.

The above solution $h_{\perp 1}(z)$ [Eq. (25)] is valid for $\alpha > 0$.

The induced image density current by the oscillating dipole is oriented in the z-direction [$j_{\perp i}(\mathbf{r},\omega)\mathbf{n}_z$]. This density current in the quasi-static approximation is

$$j_{\perp 1}(\mathbf{r},\omega) = \mathrm{i}\omega\delta(x)\delta(y)g_{\perp 1}(z). \tag{28}$$

As seen from Eqs. (28) and (26) the image distribution is: a point dipole that is located at $z = b$, and (2) a line of dipoles extending from $z = 0$ to $z = b$. Both distributions being oriented in the z-direction.

2.2.2. *Inside the sphere*

The static potential inside the sphere is (see Appendix A)

$$\Phi_{\perp 2}(r,\theta) = -\frac{p}{4\pi\varepsilon_o\epsilon_a} \times \sum_{n=0}^{\infty} \frac{\epsilon_a(2n+1)(n+1)}{(\epsilon_a+\epsilon_b)n+\epsilon_b} \frac{r^n}{z_o^{n+2}} P_n(\cos\theta). \tag{29}$$

We assume the same form for the image charge distribution as in Eq. (20), but the charge is located outside the sphere and $h_{\perp 2}$ replaces $h_{\perp 1}$. The potential created is obtained as in Eq. (21) with $h_{\perp 1}$ replaced by $h_{\perp 2}$ and the integration goes from $z = a$ to $z \to \infty$. Then, by using Eq. (22) with the substitution $u = \cos\theta$ and $v = r/z'$, the potential produced by the image charge distribution turns out to be

$$\Phi_{\perp 2}(r,\theta) = \frac{1}{4\pi\varepsilon_o\epsilon_a} \sum_{n=0}^{\infty} P_n(\cos\theta) \frac{r^n}{z_o^{n+2}} \times \int_a^{\infty} z_o h_{\perp 2}(z') \left[\frac{z_o}{z'}\right]^{n+1} dz'. \tag{30}$$

Again, by comparing Eqs. (29) and (30), we obtain that $h_{\perp 2}(z)$ must fulfill

$$\int_a^{\infty} h_{\perp 2}(z') \left[\frac{z_o}{z'}\right]^{n+1} dz' = -\frac{p}{z_o} \frac{2\epsilon_a}{\epsilon_a+\epsilon_b} \times \frac{(n+1/2)(n+1)}{n+\alpha}, \quad n = 0,1,2,\ldots \tag{31}$$

We found that the solution of Eq. (31) takes the form:

$$h_{\perp 2}(z) = \frac{d}{dz} g_{\perp 2}(z), \tag{32}$$

$$g_{\perp 2}(z) = -p\frac{2\epsilon_a}{\epsilon_a+\epsilon_b} r_2(z)\delta(z-z_o) - p\frac{\epsilon_a(\epsilon_a-\epsilon_b)}{(\epsilon_a+\epsilon_b)^2} \frac{z}{z_o^2} \left(\frac{z_o}{z}\right)^{\alpha} \Theta(z-z_o), \tag{33}$$

$$r_2 = \left(\frac{z_o}{z}\right)^{\alpha-2}. \tag{34}$$

Also, $h_{\perp 2}(z)$ is defined for $\alpha > 0$.

As the dipole oscillates, it induces the density current distribution, along the z-direction, given by

$$j_{\perp 2}(\mathbf{r},\omega) = \mathrm{i}\omega\delta(x)\delta(y)g_{\perp 2}(z). \tag{35}$$

The image charge density is constituted by: (1) an image dipole that is located at $z = z_o$, and (2) a line [from $z = z_o$ to $z \to \infty$] of dipoles that are oriented in the z-direction. This is depicted in Fig. 1c.

3. Electric Field

If a current $\mathbf{j}(\mathbf{r},\omega)$ is embedded in a nonmagnetic medium then the electric field produced by this current is given by

$$\mathbf{E}(\mathbf{r},\omega) = \mathrm{i}\mu_o\omega \int \overleftrightarrow{\mathbf{G}}(\mathbf{r},\mathbf{r}',\omega)\mathbf{j}(\mathbf{r}',\omega)d^3\mathbf{r}'. \tag{36}$$

Here, μ_o is the vacuum permeability and $\overleftrightarrow{\mathbf{G}}(\mathbf{r},\mathbf{r}',\omega)$ is the Green tensor that characterizes the electromagnetic response of an electric dipole embedded in an arbitrary environment.

The electric field created by the dipole in the vicinity of the sphere in the quasi-static approximation is

$$\mathbf{E}_{\beta i}(\mathbf{r},\omega) = \mathbf{E}_{\beta o}(\mathbf{r},\omega)\delta_{1i} + \mathbf{E}_{\mathrm{sca}\beta i}(\mathbf{r},\omega), \tag{37}$$

where $\beta = \parallel, \perp$, $i = 1$ (outside), 2 (inside), and δ is the Kronecker tensor. $\mathbf{E}_{\beta o}(\mathbf{r},\omega)$ is the electric field created by the dipole in the absence of the sphere which is

$$\mathbf{E}_{\beta o}(\mathbf{r},\omega) = \frac{k_o^2}{\varepsilon_o} \overleftrightarrow{\mathbf{G}}_1(\mathbf{r}, z_o\mathbf{n}_z, \omega)\, p\mathbf{n}_\beta, \tag{38}$$

and $\mathbf{E}_{\mathrm{sca}\beta i}(\mathbf{r},\omega)$ is the electric field created by the image currents $j_{\beta i}\mathbf{n}_\beta$ defined as

$$\mathbf{E}_{\mathrm{sca}\beta i}(\mathbf{r},\omega) = -\frac{k_o^2}{\varepsilon_o} \int \overleftrightarrow{\mathbf{G}}_i(\mathbf{r}, z'\mathbf{n}_z, \omega)\mathbf{n}_\beta\; g_{\beta i}(z')dz'. \tag{39}$$

Here, $\mathbf{n}_{\parallel(\perp)} \equiv \mathbf{n}_{x(z)}$, $k_o \equiv \omega^2/c^2$ [c is the velocity of light in a vacuum], and $\overleftrightarrow{\mathbf{G}}_{1(2)}$ is the Green's tensor for an unbounded, isotropic and nonmagnetic medium with dielectric constant $\epsilon_b(\epsilon_a)$. The explicit expression of this tensor is encountered in Appendix B.

4. Discussion of the quasi-static description

Independently of the dipole orientation, the electric field (inside or outside) arises from a point dipole and a line-current distribution. The electric field created by the point dipole resembles the quasi-static field created for a dipole in the vicinity of a planar interface. For the case of the field outside the sphere, the solution differs by a geometric weight factor (a^3/z_o^3) and the location of the image dipole.

If the radius a is large ($a \to \infty$), then we could expect that the image solution for the planar interface must be recovered. This is indeed the case. Straightforwardly, the image line contributions vanish. For the image point dipole that creates the field outside the sphere, by defining $z_o \equiv a + \Delta s$, the geometric factor $a^3/z_o^3 \to 1$ and $b \to a - \Delta s$, namely the dipole and its image are equidistant from the interface. As a consequence, the image sources are the same as those for a planar interface in this limit $a \to \infty$.

As seen in the previous section, the Green tensor has retardation. Therefore, our solution fulfills the dynamic Maxwell equations. However, the boundary conditions of the electromagnetic at the surface of the sphere are not exactly matched, since our solution comes from a static assumption. Nevertheless, the electromagnetic fields should be well approximated by using quasi-static approach in the vicinity of a small sphere ($a \ll \lambda$).

We can consider a dielectric sphere with absorption (Im$[\alpha] > 0$), but the validity of the method is assured if Re$[\alpha] + 1 > 0$ (Re$[\alpha] > 0$) for the tangential (radial) orientation.

Finally, merely as an illustration of our quasi-static method, we plot the electric field intensity $|\mathbf{E}(\mathbf{r},\omega)|^2$ generated by the dipole in the presence of a dielectric sphere for particular cases. We consider a sphere with radius $a = 30$ nm, and a dipole located at $z_o = 75$ nm and oscillating with a frequency ω corresponding to the free-space wavelength $\lambda_o = 477$ nm. We treat the cases for the sphere made of glass ($\epsilon_{gl} = 2.25$), silicon ($\epsilon_{si} = 19.72 + 0.8i$), and gold ($\epsilon_{au} = -1.7 + 4.46i$). The spheres are embedded in a vacuum ($\epsilon_b = 1$) with the exception of the gold sphere which is embedded in glass. In Fig. 3, we show the contour curves of the electric field intensity $|\mathbf{E}(\mathbf{r},\omega)|^2$ at the xz-plane for a dipole oriented in the radial direction and spheres made of glass, silicon, and gold. We note that the intensity contour curves suffer a small distortion from the presence of the glass sphere, whereas these curves are strongly distorted for the silicon and gold spheres. This is due to the fact that the scattered field by the silicon and gold particles is greater than by the glass sphere. As seen in Figs. 3b and 3c for the silicon and gold particles, the scattered field is concentrated at the left and right edges of the sphere. Since gold absorbs more energy than silicon and glass at λ_o, the gradient of the intensity $|\mathbf{E}(\mathbf{r},\omega)|^2$ inside the gold sphere is larger than in the other cases. Last, we consider the case of the dipole oriented tangentially. The contour curves of the electric field intensity $|\mathbf{E}(\mathbf{r},\omega)|^2$ at the xz-plane for this orientation are plotted in Fig. 4. Similarly to the dipole oriented radially, the distortion of intensity contour lines is more noticeable for the silicon and gold sphere than for the glass sphere. The intensity $|\mathbf{E}(\mathbf{r},\omega)|^2$ inside the sphere for the glass and silicon particles is almost homogeneous, while the opposite happens for the gold sphere (see Fig. 4). The scattered field near the sphere is concentratted predominantly on the right hand side of the sphere. Indeed, interference between the field coming directly from the dipole and the scattered electric field is appreciable in this region.

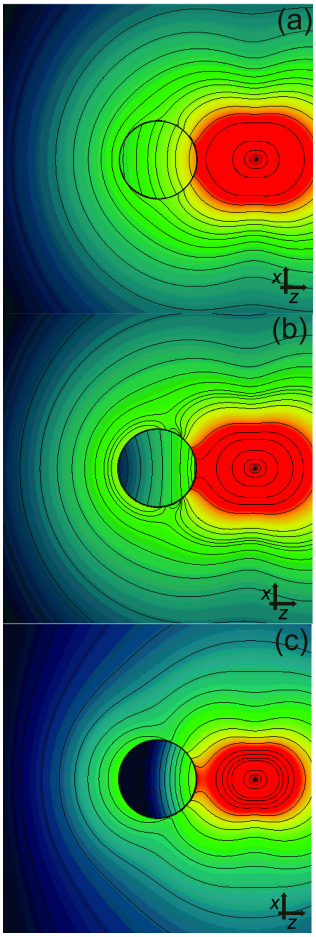

FIGURE 3. Contour curves of $\log|\mathbf{E}(\mathbf{r},\omega)|^2$ at the xz-plane for a dipole oriented in the radial direction, $z_o = 75$ nm, $a = 30$ nm, and $\lambda_o = 477$ nm. Each plot covers an area $\lambda_o/2 \times \lambda_o/2$. The color scale maps the same intensity in the plots. (a) Glass sphere (dielectric) embedded in vacuum ($\epsilon_b = 1$). (b) Silicon sphere (semiconductor) embedded in vacuum ($\epsilon_b = 1$). (c) Gold sphere (metal) embedded in glass $\epsilon_b = 2.25$.

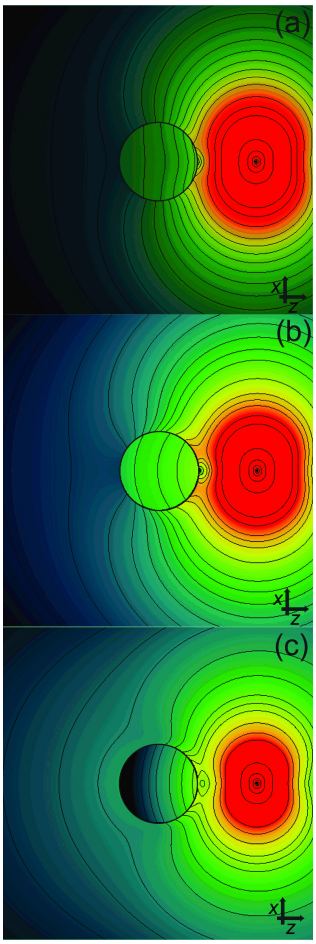

FIGURE 4. Contour curves of $\log|\mathbf{E}(\mathbf{r},\omega)|^2$ at the xz-plane for a dipole oriented in the tangential direction, $z_o = 75$ nm, $a = 30$ nm, and $\lambda_o = 477$ nm. Each plot covers an area $\lambda_o/2 \times \lambda_o/2$. The color scale maps the same intensity for the plots. (a) Glass sphere (dielectric) embedded in vacuum ($\epsilon_b = 1$). (b) Silicon sphere (semiconductor) embedded in vacuum ($\epsilon_b = 1$). (c) Gold sphere (metal) embedded in glass $\epsilon_b = 2.25$.

5. Conclusions

We presented a quasi-static description in which the electromagnetic fields that are created by an oscillating dipole arise from image sources. We derived the expressions of the image sources for the principal orientations (tangential and radial). We found that the current image source for these orientations is constituted by a point dipole and a line current. A simple physical picture for the response of the electric dipole in the vicinity of the sphere was obtained. The quasi-static electromagnetic fields produced by the dipole are obtained from the Green tensor for a bulk material. The contribution of the field arising from the line current is obtained by performing a single quadrature integral. To illustrate our method, we obtained plots of the electric field created by an electric dipole for particular cases.

This method can be applied to study the electromagnetic response of emitters near a dielectric nano-sphere.

Appendix

A. Potential inside sphere

Herein, we derive the potential in $\Phi_{\beta,2}$ ($\beta = \perp, \parallel$) from the potential created by a single charge q placed outside the sphere at $z_o\mathbf{n}_z$ which is given by [12]

$$\phi_{\text{in}}(r,\theta) = \frac{q}{4\pi\varepsilon_o} \times \sum_{n=0}^{\infty} \frac{2n+1}{(\epsilon_a+\epsilon_b)n+\epsilon_b} \frac{r^n}{z_o^{n+1}} P_n(\cos\theta). \quad \text{(A.1)}$$

The potential inside the sphere can be obtained from Eq. (A.1) as:

$$\Phi_{\perp 2}(r,\theta) = \frac{p}{q}\frac{\partial}{\partial z_o}\phi_{\text{in}}(r,\theta), \quad \text{(A.2)}$$

$$\Phi_{\parallel 2}(r,\theta,\phi) = \frac{p}{qz_o}\frac{\partial}{\partial\theta_o}\phi_{\text{in}}(r,\xi)\Big|_{\theta_o=0}, \quad \text{(A.3)}$$

where

$$\cos\xi = \cos\theta\cos\theta_o + \sin\theta\sin\theta_o\cos\phi. \quad \text{(A.4)}$$

To obtain the final expression for $\Phi_{\parallel 2}$, we use the fact that

$$P_n^1(y) = (1-y^2)^{1/2}\frac{d}{dy}P_n(y). \quad \text{(A.5)}$$

B. Green tensor for a bulk medium

The Green tensor in a bulk material with dielectric constant $\epsilon(\omega)$ can be expressed as

$$\overleftrightarrow{\mathbf{G}}(\mathbf{r},\mathbf{r}',\omega) = \overleftrightarrow{\mathbf{G}}_{\text{nf}}(\mathbf{r},\mathbf{r}',\omega) + \overleftrightarrow{\mathbf{G}}_{\text{if}}(\mathbf{r},\mathbf{r}',\omega) + \overleftrightarrow{\mathbf{G}}_{\text{ff}}(\mathbf{r},\mathbf{r}',\omega), \quad \text{(B.1)}$$

where $\overleftrightarrow{\mathbf{G}}_{\text{nf}}(\mathbf{r},\mathbf{r}',\omega)$, $\overleftrightarrow{\mathbf{G}}_{\text{if}}(\mathbf{r},\mathbf{r}',\omega)$, and $\overleftrightarrow{\mathbf{G}}_{\text{ff}}(\mathbf{r},\mathbf{r}',\omega)$ are the nearfield, intermediate-field, and farfield contributions, respectively. These partial contributions are defined as

$$\overleftrightarrow{\mathbf{G}}_{\text{nf}}(\mathbf{r},\mathbf{r}',\omega) = \frac{e^{ikR}}{4\pi R}\frac{1}{k^2R^2}\left[-\overleftrightarrow{\mathbf{I}} + 3\mathbf{n}_{\text{R}}\mathbf{n}_{\text{R}}\right], \quad \text{(B.2a)}$$

$$\overleftrightarrow{\mathbf{G}}_{\text{if}}(\mathbf{r},\mathbf{r}',\omega) = \frac{e^{ikR}}{4\pi R}\frac{-i}{kR}\left[-\overleftrightarrow{\mathbf{I}} + 3\mathbf{n}_{\text{R}}\mathbf{n}_{\text{R}}\right], \quad \text{(B.2b)}$$

$$\overleftrightarrow{\mathbf{G}}_{\text{ff}}(\mathbf{r},\mathbf{r}',\omega) = \frac{e^{ikR}}{4\pi R}\left[\overleftrightarrow{\mathbf{I}} - \mathbf{n}_{\text{R}}\mathbf{n}_{\text{R}}\right]. \quad \text{(B.2c)}$$

Here, $k = \omega\sqrt{\epsilon(\omega)}/c$, $R = |\mathbf{r}-\mathbf{r}'|$, $\mathbf{n}_{\text{R}} = (\mathbf{r}-\mathbf{r}')/R$, and $\overleftrightarrow{\mathbf{I}}$ is the unit dyadic.

1. H. Chew, *J. Chem. Phys.* **87** (1987) 1355.
2. I.V. Lindell, *Am. J. Phys.* **61** (1993) 39.
3. E. Betzig and R.J. Chichester, *Science* **262** (1993) 1422.
4. E.J. Sánchez, L. Novotny, and X.S. Xie, *Phys. Rev. Lett.* **82** (1999) 4014.
5. J. Gersten and A. Nitzan, *J. Chem. Phys.* **75** (1981) 1139.
6. R. Ruppin, *J. Chem. Phys.* **76** (1982) 1681.
7. P. Anger P. Bharadwaj and L. Novotny, *Phys. Rev. Lett.* **96** (2006) 113002.
8. F. Cannone, G. Chirico, A.R. Bizzarri, and S. Cannistraro, *J. Phys. Chem. B* **110** (2006) 16491.
9. S. Kühn, U. Håkanson, L. Rogobete, and V. Sandoghdar, *Phys. Rev. Lett.* **97** (2006) 017402.
10. G.W. Ford and W.H. Weber, *Phys. Rep.* **113** (1984) 195.
11. G.B. Arfken and H.J. Weber, *Mathematical Methods for Physicists*, ed. 5th (Academic Press, San Diego, 2001),
12. J.A. Stratton, *Electromagnetic Theory* (McGraw-Hill, New York, 1941).